Author(s): Loh, E.W.K; Wijeyesekera, D. Chitral
Article title: Drying Kinetic of Prehydrated and Extruded Clay Mat
Year of publication: 2009
Citation: Loh, E.W.K. and Wijeyesekera, D.C. (2009) 'Drying Kinetic of Prehydrated and Extruded Clay Mat' Proceedings of the AC&T, pp. 95-101.
Link to published version:
http://www.uel.ac.uk/act/proceedings/documents/FinalProceedings.pdf

DRYING KINETIC OF PREHYDRATED AND EXTRUDED CLAY MAT

E.W.K.Loh and D.C.Wijeyesekera
Built Environment Research Group
ericwkloh@uel.ac.uk; d.c.wijeyesekera@uel.ac.uk

Abstract: The isothermal drying of prehydrated and extruded clay mat was investigated on a laboratory scale over a temperature and relative humidity range from 20°C to 40°C and 15% to 70% respectively. Two sets of polymer enhanced clay mats were used in this study. By measuring the mass loss of the samples during the isothermal drying process basis dependencies necessary to describe the kinetic drying process was obtained. The most commonly used model, Page, Wang & Singh, Henderson & Pabis and Thin layer equation were used to fit experimental data using a non-linear regression analysis. The fit quality of the proposed model was evaluated by using the standard error of estimate, relative percent error and coefficient of correlation. Results probed that the Page model was more appropriated to predict prehydrated and extruded clay mat for the range of temperatures and relative humidity studied. Applied model analysis enabled evaluation of the main transport properties: drying constant, drying rate, effective diffusion coefficient and exponential model parameter. It was found that the drying condition and type of polymer incorporated in the clay mat strongly influenced the drying kinetic and transport parameters.

1. Introduction:

The clay drying process plays an important role in manufacturing process of numerous commercial materials like: ceramic, tilery, brick yards, pottery etc. As of recent times, factory prehydrated bentonite clay mats are used in the form of composite contaminant barriers or as structural waterproofing in the construction industry. From a quality control perspective, this 'unique' prehydration needed to be sustained at appropriate moisture condition to facilitate the rolling process and allows sufficient integral tensile strength. It is also critical that the consistency of the clay is preserved to ensure that the mat remains flexible with no possibility of it developing brittle fractures in a hostile thermal environment.

In order understand the drying characteristic of the clay mat in different thermal environment, it is essential and useful to propose some descriptive mathematical models which include the evaluation of the key process drying parameters.

2. Materials and Methods:

2.1. Samples Properties:

Two sets of clay mats, namely TSA and TSB were used in the experimental measurements. TSA and TSB were polymer treated and vacuum extruded bentonite. One of the primary purposes of the liquid polymer treatment is to improve the mechanical properties of the clay mats.

The X-ray diffraction (XRD) analysis showed the clay mineralogy of the bentonite to be smectite (93%), quartz (2%), feldspars (4%) and gypsum (1%). Bulk sample is composed of 87.5% of particles in a size range less than 75μm and air dried moisture content of 10 -14% by weight.

The experiments were performed in an environmental chamber with controllable temperature and relative humidity. A 5mm thick sample with a diameter of 100mm was placed on the sample holder and allowed to dry isothermally under preset conditions. The mass evolution from the sample with time was monitored using a digital balance linked to a computer facilitating regular data acquisition. Air temperature and relative humidity are measured by a thermo-hygrometer. The accuracy of measurement is as follows: 0.01g for mass, 0.1ºC for temperature and 0.1% for the relative humidity.

2.2. Mathematical Model:

The experimentally obtained data were correlated with the following different mathematical models:

i. **Wang & Singh (Wang & Singh, 1978)**

$$X = \left(X_0 - X_{eq}\right)\left(1 + at + bt^2\right) + X_{eq} \qquad (1)$$

ii. **Henderson & Pabis (Guarte, 1996)**

$$X = \left(X_0 - X_{eq}\right).\beta e^{-k.t} + X_{eq} \qquad (2)$$

iii. **Thin layer equation (Jayas, 1991)**

$$X = \left(X_0 - X_{eq}\right).e^{-k.t} + X_{eq} \qquad (3)$$

iv. **Page (Jayas, 1991)**

$$X = \left(X_0 - X_{eq}\right).e^{-k.t^n} + X_{eq} \qquad (4)$$

In order to establish the most appropriate applied models for the experimental data, a non-linear least squares regression analysis was used to fit the experimental data. A SigmaPlot® graphing software from SYSTAT was undertaken for this purpose.

The quality of the fitting was evaluated by calculating the mean relative percent error (P), standard error (SE) and the coefficient of correlation (R^2) between the experimental (y_{exp}) and predicted data (y_{cal}). That is:-

$$P = \frac{100}{N}\sum_{j=1}^{N}\left|\frac{y_{jcal} - y_{j\exp}}{y_{j\exp}}\right| \qquad (5)$$

$$SE = \sqrt{\sum_{j=1}^{N}\frac{\left(y_{jcal} - y_{j\exp}\right)^2}{N - n_p}} \qquad (6)$$

$$R^2 = \frac{S_t - SSE}{S_t} \qquad (7)$$

where,

$$S_t = \sqrt{\frac{\sum_{j=1}^{N}\left(\bar{y} - y_j\right)^2}{n-1}} \qquad (8)$$

$$\bar{y} = \frac{\sum_{j=1}^{N} y_j}{N} \qquad (9)$$

$$SSE = \sum_{j=1}^{N}\left(y_{jcal} - y_{j\exp}\right)^2 \qquad (10)$$

3. Results and Discussion:

3.1. Best Fit Drying Kinetic Models:

Experimental data for TSA sample obtained from the ‘B2’ environmental condition (temperature = 30°C and relative humidity = 50%) was chosen and the observed outputs for this condition are presented in this paper. The parameters derived in Table 1 demonstrated that all models give a good fit ($0.9924 < R^2 < 0.9998$) to the experimental data with R^2 value very close to 1. The standard error and mean relative error for Wang & Singh model is 0.5821 and 2.0541;

Table 1 Statistical parameters and comparison criteria for different kinetic model

Parameter	**Model**				**For Perfect Fit**
	Wang & Singh (Wang & Singh, 1978)	**Henderson & Pabis** (Guarte, 1996)	**Thin Layer equation** (Jayas, 1991)	**Page** (Jayas, 1991)	
SSR	38092.1443	38316.2598	38316.2598	38377.1441	**-**
SSE	291.7321	67.6166	67.6166	6.7323	**0.00**
S_t	38383.8764				**-**
(%P)	2.0541	0.8806	0.8806	0.3452	**0.00**
SE	0.5821	0.2802	0.2801	0.0884	**0.00**
R^2	0.9924	0.9982	0.9982	0.9998	**1.00**

and the coefficient of correlation R^2 value between the experimental value and predicted value is 0.9924.

It is note worthy that for the Henderson & Pabis model and Thin Layer equation, the same values of 0.8806 and 0.9982 are obtained for *%P* and R^2 parameter respectively; and the difference in standard error is insignificant. This suggests that the free parameter β is not needed.

From an overall view point, the Page model gave the most desirable *%P*, *SE* and R^2 values compared to the other models. The highest coefficient of correlation R^2 value (0.9998) as well as the lowest *%P* (0.3452) and *SE* (0.0884) value made it favourable to be the most appropriate regression model.

3.2. Drying Constants:

The drying constants k and n in the Page equation are essentially functions of transport properties. The influence of the thermal environment condition on these parameters is analyzed and presented in Table 2 for TSA and TSB samples respectively.

For a given temperature, an increase in the relative humidity causes a reduction of parameter k. This phenomenon is more pronounced in the higher temperature range. Conversely, the sensitivity of parameter k to temperature apparently reveals that at a lower relative humidity range. It was observed that the increase in temperature leading to an increase in the parameter k.

It was no significant dependency between parameter n on the thermal environment can be noted from the present study. This similar observation was also reported by Sander et al. (1998 & 2003) for thin plates of illite montmorillonite clay. Sander had concluded that the parameter n is independent to the drying condition.

Although the ranges of the parameter k (0.001 to 0.007) and parameter n (0.60 to 0.95) for the TSA and TSB samples are very similar, their distribution are different over the range of temperature $(20°C \leq T \leq 40°C)$ and relative humidity $(30\% \leq T \leq 70\%)$.

Table 2 Estimated parameter k and n for TSA mixed and TSB mixed samples

		Sample Type			
		TSA		**TSB**	
Thermal Environment		**k [min^{-1}]**	**n [-]**	**k [min^{-1}]**	**n [-]**
A1	Temperature = 20°C Relative Humidity = 30%	0.002038	0.7960	0.000875	0.8750
A2	Temperature = 20°C Relative Humidity = 50%	0.001851	0.7742	0.001656	0.7975
A3	Temperature = 20°C Relative Humidity = 70%	0.001597	0.7501	0.000013	0.8327
B1	Temperature = 30°C Relative Humidity = 30%	0.003646	0.7592	0.002295	0.7916
B2	Temperature = 30°C Relative Humidity = 50%	0.002401	0.7796	0.000800	0.8569
B3	Temperature = 30°C Relative Humidity = 70%	0.002162	0.6625	0.000234	0.6745
C0	Temperature = 40°C Relative Humidity = 15%	0.004521	0.7671	0.005947	0.6692
C1	Temperature = 40°C Relative Humidity = 30%	0.003158	0.7960	0.003494	0.7573
C2	Temperature = 40°C Relative Humidity = 50%	0.001700	0.8287	0.000690	0.9423
C3	Temperature = 40°C Relative Humidity = 70%	0.000573	0.9455	0.000588	0.9571

3.3. Moisture Diffusion Coefficient:

For a drying process where the absence of a constant rate period is observed, such as in the present case, then it could be assumed that internal diffusion prevails as a mechanism of matter transfer. Therefore, moisture diffusivity can be calculated from the experimental drying data using Fick's second law (Sander et al., 1998).

According to Geankoplis (1983), the solution to the diffusion equation for thin plate shaped material drying from one surface is:

$$\psi = \frac{X - X_{eq}}{X_0 - X_{eq}} = \frac{8}{\pi^2} \cdot e^{\left(\frac{-\pi^2 \cdot D_{eff} \cdot t}{L^2}\right)} \qquad (11)$$

Equation 11 can be approximated to a linear form, which is convenient for determining effective diffusion coefficient, in the manner show in Equation 12.

$$\ln\psi = \ln\frac{8}{\pi^2} - \frac{\pi^2 \cdot D_{eff}}{L^2}\cdot t \qquad (12)$$

By presenting the dependence between the dimensionless moisture content on drying time in a semilog graph as shown in Figure 1, straight lines are obtained from which the slope, the effective diffusion coefficient is calculated and presented in Table 3.

It is evident that the effective diffusion coefficient is dependent on the drying temperature. The higher temperature gives a higher value for the effective diffusion coefficient. Contrarily, an increase in the relative humidity level results in a reduction in the effective diffusion coefficient. This observation is further supported by the evidence from the drying kinetic model as shown in Figure 2. The drying kinetics increase with the air temperature due to an increase in the convective heat flux transport brought about by the air to the sample. The acceleration of the internal moisture migration, leads to an increase of the effective diffusion coefficient value. Conversely, an increase in the relative humidity causes a reduction of the isenthalpic flux. The critical moisture content corresponding to the drying regime change of varies in the same way. The equilibrium moisture content increases naturally with an increase of the relative humidity level.

Comparing the effective diffusion coefficient obtained with the TSA and TSB samples, it is evident that they differ substantially under similar thermal environment conditions. It is observed that with TSA sample, the moisture diffusivity is higher and this trend is consistent with the experimental observations. A plausible explanation for this deviation is the consequence of the higher biding energy of the polymer properties in TSB sample. This finding is further supported by the evidence from desorption isotherm model reported in Loh & Wijeyesekera (2008).

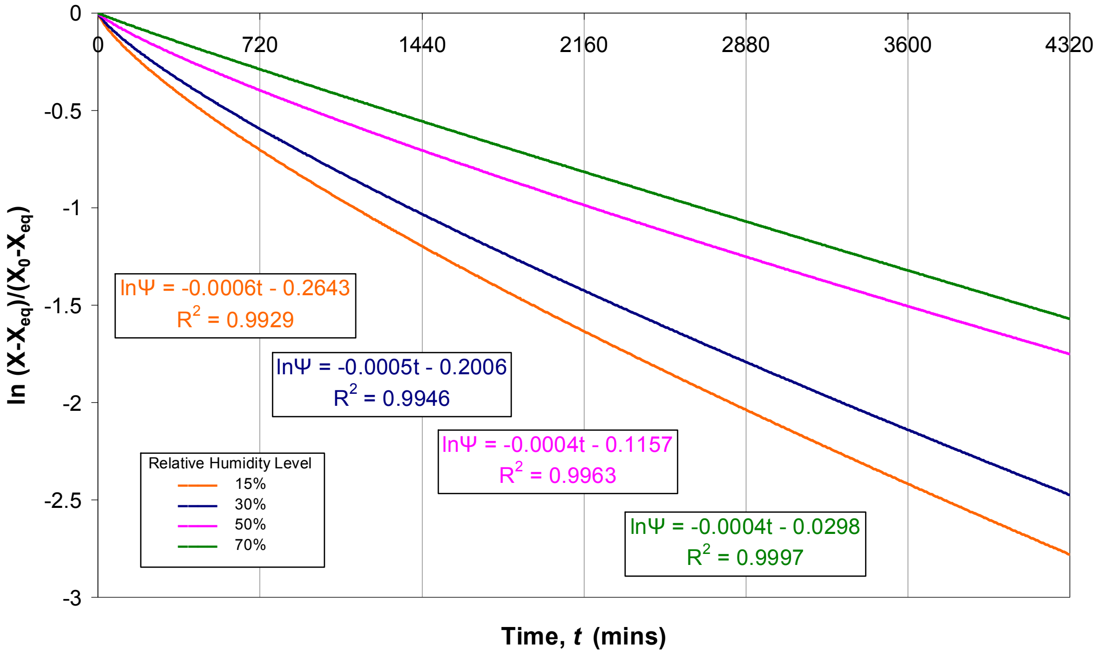

Figure 1 Moisture diffusivity of TSA sample at 40°C environment conditions

Table 3 Estimated effective diffusion coefficients, D_{eff} for TSA and TSB samples

		Sample Type	
		TSA	**TSB**
Thermal Environment		D_{eff} [m^2 min^{-1}]	D_{eff} [m^2 min^{-1}]
A1	Temperature = 20°C Relative Humidity = 30%	1.01×10^{-9}	7.60×10^{-10}
A2	Temperature = 20°C Relative Humidity = 50%	7.60×10^{-10}	7.60×10^{-10}
A3	Temperature = 20°C Relative Humidity = 70%	5.07×10^{-10}	7.60×10^{-12}
B1	Temperature =30°C Relative Humidity = 30%	1.27×10^{-9}	1.01×10^{-9}
B2	Temperature =30°C Relative Humidity = 50%	1.01×10^{-9}	5.07×10^{-10}
B3	Temperature =30°C Relative Humidity = 70%	2.53×10^{-10}	2.53×10^{-11}
C0	Temperature =40°C Relative Humidity = 15%	1.52×10^{-9}	1.27×10^{-9}
C1	Temperature =40°C Relative Humidity = 30%	1.27×10^{-9}	1.01×10^{-9}
C2	Temperature = 40°C Relative Humidity = 50%	1.01×10^{-9}	1.01×10^{-9}
C3	Temperature =40°C Relative Humidity = 70%	1.01×10^{-9}	1.01×10^{-9}

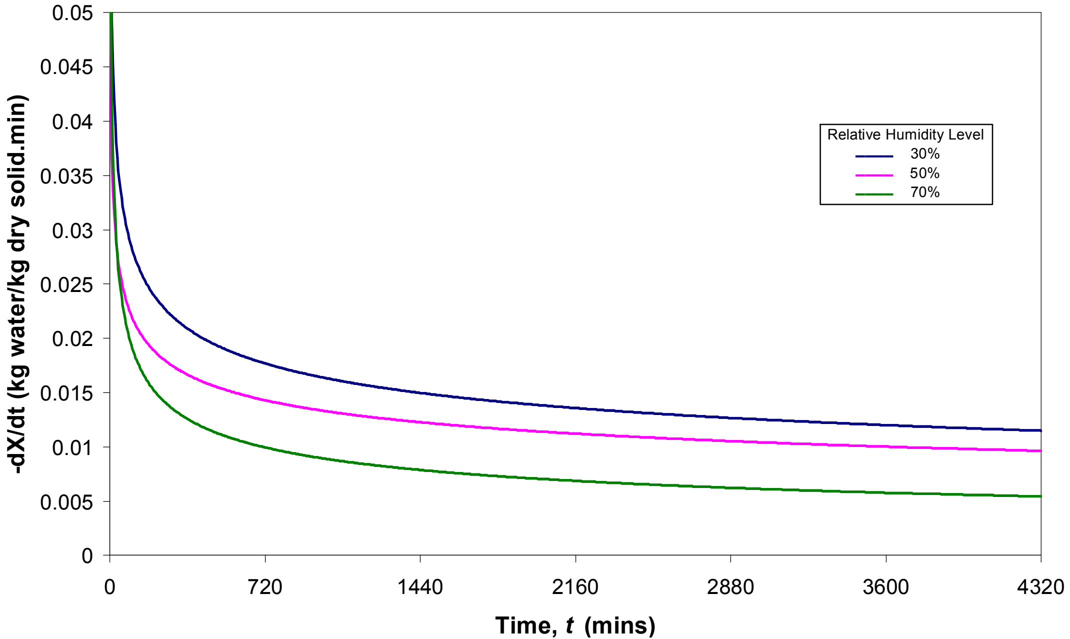

Figure 2 Drying-rate curves for the TSA sample at 30°C environment conditions

4. Conclusion:

In order to study the drying characteristic of the prehydrated and extruded clay mat in varies thermal environment, kinetic of isothermal convection drying were investigated.

High correlation between Page model and experimental data justifies the applied mathematical model for describing the drying kinetic in isothermal condition.

The influence of temperature and relative humidity level on the transport properties: drying constant, drying rate, effective diffusion coefficient and exponential model parameter were estimated.

It was found that the drying rate and moisture diffusion coefficient are also dependent on the material properties, such as the capability to retard moisture movement in the TSB sample compared to the TSA sample.

5. Notations:

D_{eff} - effective diffusivity at the drying temperature [m^2/s]
k - parameter in Model [s^{-1}]
L - thickness of the slices [m]
n - parameter in Model [s^{-1}]
t - drying time [s]
X - moisture content [%]
X_0 - initial moisture content [%]
X_{eq} - equilibrium moisture content [%]
ψ - dimensionless moisture content

6. References:

Geankoplis, C.J., (1993) *Transport Processes and Unit Operation*, 3rd Edition, Prentice Hall, Englewood Cliffs.

Guarte RC. (1996) *Modelling the drying behaviour of copra and development of a natural convection dryer for production of high quality copra in the Philippines*. Ph.D. thesis, Hohenheim University, Germany.

Jayas, D.S., Cenkowski, S., Pabis, S. & Muir, W.E. (1991) Review of thin-layer drying and wetting equations. *Drying Technology*, 9(3), 551-588.

Loh, E.W.K. and Wijeyesekera, D.C.(2008). Moisture Desorption Isotherms and Thermodynamic Characteristic of Prehydrated and Extruded GCL. In *proceedings of the Advances in Computing and Technology*, The School of Computing and Technology 3rd Annual Conference, University of East London, UK.

Sander, A., Skansi, D. & Bolf, N. (2003). Heat and mass transfer models in convection drying of clay slabs. *Ceramics International*, 29(6), 641–653

Sander, A., Tomas, S. & Skansi, D. (1998). The influence of air temperature on effective diffusion coefficient of moisture in the falling rate period. *Drying Technology*, 16(7), 1487-1499.

Wang, C.Y. & Singh, R.P. (1978) A single layer drying equation for rough rice. *ASAE Paper No. 3001. St.Joseph*.